

PREDICTIVE CONTROL OF DOUBLY FED INDUCTION GENERATOR USED FOR WIND ENERGY

Omar FEZAZI Ahmed MASSOUM

Djillali Liabes University of Sidi Bel Abbas

fezazi-omar@hotmail.com ahmassoum@yahoo.fr

Abstract: When the system is non-linear and the parameters of the model are changing in large proportions, the classic controller (PID) is not satisfying; so in this paper we recall generalized predictive control (GPC) for doubly fed induction generation (DFIG) used for wind turbine. First a mathematical model of the machine is written in an appropriate d-q reference then we used the GPC controller to control the active and reactive power. We conclude with a simulation by MATLAB SIMULINK to see responses of our machine and performance of GPC control.

Key words: Modeling, simulation, DFIG, GPC, predictive control

1. Introduction

Electricity has become indispensable for humanity; because guarantee better living conditions so the global needs of electricity is growing day by day. For these reasons and the problem of environmental pollution many countries tended to use the renewable energy among these wind energy appears the global wind power capacity installed in the world 369,597 MW.

The wind potential in Algeria differs by location knowing that Adrar region is located in a wind corridor of 6 m / s and extends up to 20 m / s while in In Amenas the wind speed is 6 m / s up to 14 m / s.

In this paper, we will try to model a wind turbine mechanical parts and electrical parts (generator). So we will use the most used generator for wind conversion technology the Doubly Fed Induction Generator. So we will try to model and control this generator (DFIG) of a power of 1,5MW.

The DFIG stator is directly connected to the grid and the rotor is also connected to the grid but via a transformer and a 2 level inverter the rotor-side converter controls the active and reactive power.

We're going to model our generator passing the three-phase machine model to a simpler biphasic model equivalent to control active and reactive power independently.

The generalized predictive control is one of the new most interesting solutions to implant during this last decade. By this control we can obtain many desired performances in the presence of disturbances

and the internal variations, so we used it in many applications in different field.

The principle of predictive control is to predict the value that should take output signal of the system and deduce the control leading to these values or use a dynamic model of the system inside the controller in real time to anticipate the future behavior of the system.

The implementation of this command requires [24] first setting a digital model of the system allowing to make the prediction, this model can be obtained by a discretization of continuous transfer function of the model (z-transform), then development of a sequence of future orders, It is obtained by minimization of a quadratic cost function on a finite horizon, then based on the principle of the receding horizon which is based by applying to the system only by the first control signal value.

Finally, in our study we implemented our GPC to control active and reactive powers and use MATLAB Simulink to see the performance of our mode of control In terms of reference tracking, and robustness after changing of parameter of the DFIG in case of faults change of resistance after changing the coil temperature change of inductance after changing the coil temperature because of saturation of the magnetic field.

2. Modeling of the wind turbine

We are going to model all part of the turbine, the blades multiplier and mechanical shaft that will train our generator, it will be assumed that the wind has a fixed speed $V= 12m / s$; the three blades have the same inertia, the same elasticity and the same coefficient of friction and the distribution of the wind speed is uniform over all the blades.

2.2. Aerodynamic model of the blades

The turbine, which will be modeled, has three adjustable blades with length R fixed to a drive shaft turning at a speed Ω_r which turns a generator by a multiplier the kinetic power of the wind through the wind disc [1-16-17]:

$$P_v = \frac{1}{2} \rho \pi R V^3 \quad (1)$$

The wind turbine cannot recover all the power of wind and aerodynamic power appearing at the rotor of the turbine is then:

$$P_t = C_p P_v = \frac{1}{2} \rho \pi R^2 v^3 C_p(\lambda, \beta) \quad (2)$$

With the relative speed $\lambda = \frac{\Omega R}{v}$

The torque exerted by the wind on the turbine shaft

$$C_t = \frac{P_v}{\Omega} = \frac{1}{2} \rho \pi R^3 v^2 C_c(\lambda, \beta) \quad (3)$$

With the torque coefficient: $C_c = \frac{C_p}{\lambda}$

2.3. Analytical model of the power coefficient

The power coefficient C_p depends on the number of the rotor blades and their geometric shapes and aerodynamic, we use an approximate expression of the power coefficient depending on the relative speed λ and the pitch angle β of the blades whose expression originates work Siegfried Heier[22]:

$$C_p(\lambda, \beta) = 0.5 \left[\frac{116}{\lambda_i} - 0.4\beta - 5 \right] \exp \left[\frac{-21}{\lambda_i} \right] + 0.0068\lambda \quad (4)$$

With $\frac{1}{\lambda_i} = \frac{1}{\lambda + 0.08\beta} - \frac{0.035}{\beta^3 + 1}$

The figure (1) shows the simulation results in MATLAB/Simulink of evolution of power coefficient C_p a function of the relative speed λ for different pitch angles β .

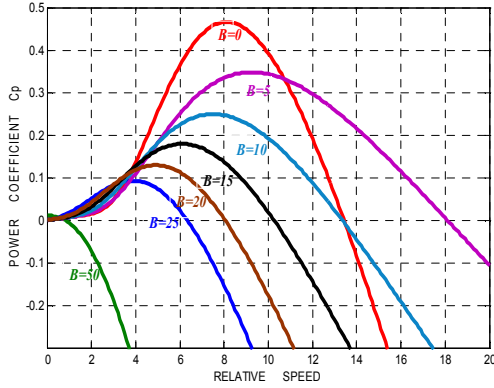


Fig. 1. The evolution of power coefficient C_p

From the figure (1) it can be seen that for each pitch angle β there is an optimum relative speed λ which maximizes the coefficient C_p . We also can see that the C_p coefficient reaches a maximum $C_{p_{\max}} = 0.48$ for a pitch angle $\beta = 0^\circ$ and a particular value of the speed ratio which is designated $\lambda_{opt} = 8.1$

Knowing the speed of the turbine the aerodynamic

torque is determined by [1-2]:

$$C_t = \frac{P_t}{\Omega_t} = \left(\frac{C_p (\rho S V_v^3)}{2} \right) * \left(\frac{1}{\Omega_{twb}} \right) \quad (5)$$

The multiplier is mathematically modeled by the following equations:

$$C_g = \frac{C_t}{G} \quad (6)$$

$$\Omega_t = \frac{\Omega_g}{G} \quad (7)$$

The connection between the turbine and the electric part of the wind is represented here by the equation of the shaft

$$J = \frac{J_t}{G^2} + J_g \quad (8)$$

Mechanical torque applied to the rotor

$$\frac{Jd\Omega_g}{dt} = C_{mec} = C_g - C_{em} - C_f \quad (9)$$

And we have that:

$$C_f = f \Omega_g \quad (10)$$

Figure (2) represents the block diagram of the model of the turbine and figure (3) represents pitch control implemented in environment MATLAB / Simulink

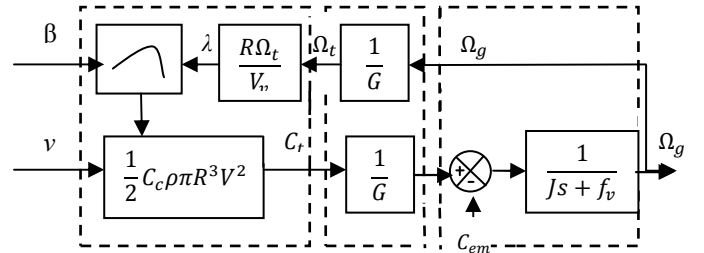


Fig. 2. Block diagram of the model of the turbine

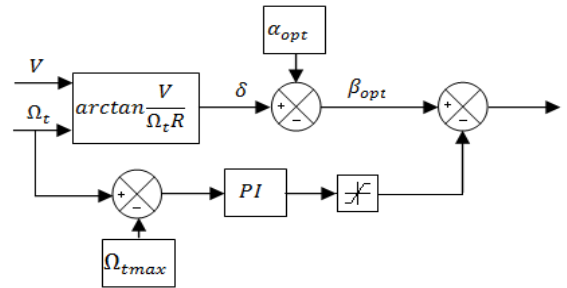


Fig. 3. Block diagram of pitch control

The relative angle

$$\delta = \arctan \frac{\Omega_t R}{V} \quad (11)$$

The angle of incidence α of the relative wind is

$$\alpha = \delta + \beta \quad \text{so} \quad \beta_{opt} = \delta - \alpha_{opt} \quad (12)$$

3. Modeling of doubly fed induction generator

For the choice of electric generator we have a generator that will allow us to independently control both active and reactive powers

Double fed induction generator (DFIG) allows us optimal production of electricity whatever wind speed and provides a rotational speed variation of $\pm 30\%$ around the synchronous speed.

The DFIG has a competitive price and superior strength and has several modes of engine operation motor hypo and hyper synchronous generator hypo and hyper synchronous but only the synchronous mode with the stator directly connected to the network and the twisted powered by an inverter we are concerned in our study.

The modeling of the DFIG is described in the d-q Park reference frame. The following equations systems describe the total generator model [1-5-15].

We deduce transformation for voltages:

$$V_{ds} = R_s I_{ds} + \frac{d\phi_{ds}}{dt} - \dot{\theta}_s \phi_{qs} \quad (13)$$

$$V_{qs} = R_s I_{qs} + \frac{d\phi_{qs}}{dt} + \dot{\theta}_s \phi_{ds} \quad (14)$$

$$V_{dr} = R_r I_{dr} + \frac{d\phi_{dr}}{dt} - \dot{\theta}_r \phi_{qr} \quad (15)$$

$$V_{qr} = R_r I_{qr} + \frac{d\phi_{qr}}{dt} + \dot{\theta}_r \phi_{dr} \quad (16)$$

$$\phi_{ds} = L_s I_{ds} + M I_{dr} \quad (17)$$

$$\phi_{qs} = L_s I_{qs} + M I_{qr} \quad (18)$$

$$\phi_{dr} = L_r I_{dr} + M I_{ds} \quad (19)$$

$$\phi_{qr} = L_r I_{qr} + M I_{qs} \quad (20)$$

Mechanical, active and reactive power equations for DFIG are:

$$\Gamma_{em} = \Gamma_r + f \Omega + \frac{Jd\Omega}{dt} \quad (21)$$

$$P_s = -V_s \frac{M}{L_s} I_{qr} \quad (22)$$

$$Q_s = -V_s \frac{M}{L_s} I_{dr} + \frac{V_s^2}{L_s \omega_s} \quad (23)$$

Resulting general model of our generator:

$$V_{dr} = R_r I_{dr} + \left(L_r - \left(\frac{M^2}{L_s} \right) \right) \frac{dI_{dr}}{dt} - \quad (24)$$

$$-g \left(L_r - \left(\frac{M^2}{L_s} \right) \right) \omega_s I_{qr}$$

$$V_{qr} = R_r I_{qr} + \left(L_r - \left(\frac{M^2}{L_s} \right) \right) \frac{dI_{qr}}{dt} - \quad (25)$$

$$-g \left(L_r - \left(\frac{M^2}{L_s} \right) \right) \omega_s I_{qr} + \frac{g(MV_s)}{L_s}$$

The principle of predictive control is to predict the values that should be the output of the system and to deduce the order leading to these values or use a dynamic model of the system within the real-time controller to anticipate the future behavior of the system.

The implementation of this control needs following points:

Definition of a numerical model of the system to realize the prediction of future behavior of the system;

Development of a sequence of future orders;

The principle of receding horizon that only the first element of the optimal control sequence is applied to the system;

To define the criterion requires horizons of four parameters of adjustment:

N_1 : Initialization horizon, N_2 : Prediction horizon

N_u : Control horizon λ : Control weighting coefficient

4. Modeling the 2 level inverter

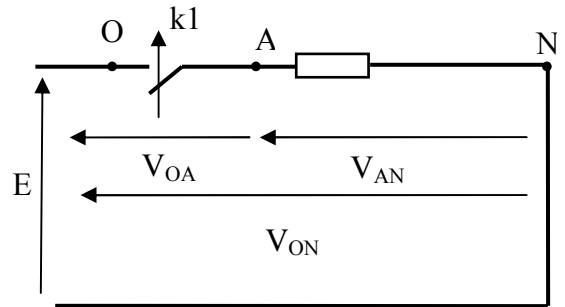


Fig. 4. Diagram of one phase of the inverter

Determining simple voltage equations applied to three stator phases.

According to the scheme equivalent deduced:

$$\begin{cases} V_{ON} = V_{OA} + V_{AN} & \text{phase A} \\ V_{ON} = V_{OB} + V_{BN} & \text{phase B} \\ V_{ON} = V_{OC} + V_{CN} & \text{phase C} \end{cases} \quad (26)$$

$$\begin{cases} V_{AN} = V_{ON} - V_{OA} & \text{phase A} \\ V_{BN} = V_{ON} - V_{OB} & \text{phase B} \\ V_{CN} = V_{ON} - V_{OC} & \text{phase C} \end{cases} \quad (27)$$

So the voltages applied to the three stator phases are:

$$\begin{cases} V_{AN} = V_{AO} + V_{ON} \\ V_{BN} = V_{BO} + V_{ON} \\ V_{CN} = V_{CO} + V_{ON} \end{cases} \quad (28)$$

So we will find that:

$$V_{AN} + V_{BN} + V_{CN} = V_{AO} + V_{BO} + V_{CO} + 3V_{ON} \quad (29)$$

With

$$V_{AN} + V_{BN} + V_{CN} = 0 \quad (30)$$

So

$$V_{AO} + V_{BO} + V_{CO} + 3V_{ON} = 0 \quad (29)$$

So:

$$V_{ON} = -\frac{1}{3}(V_{AO} + V_{BO} + V_{CO}) \quad (31)$$

We replace (31) in (29) we have the following system

$$\begin{cases} V_{AN} = \frac{2}{3}V_{AO} - \frac{1}{3}V_{BO} - \frac{1}{3}V_{CO} \\ V_{BN} = -\frac{1}{3}V_{AO} + \frac{2}{3}V_{BO} - \frac{1}{3}V_{CO} \\ V_{CN} = -\frac{1}{3}V_{AO} - \frac{1}{3}V_{BO} + \frac{2}{3}V_{CO} \end{cases} \quad (32)$$

We can write the above system in matrix form:

$$\begin{bmatrix} V_{AN} \\ V_{BN} \\ V_{CN} \end{bmatrix} = \frac{1}{3} \begin{bmatrix} 2 & -1 & -1 \\ -1 & 2 & -1 \\ -1 & -1 & 2 \end{bmatrix} \begin{bmatrix} V_{AO} \\ V_{BO} \\ V_{CO} \end{bmatrix} \quad (33)$$

$$\text{With: } \begin{cases} V_{AO} = ES_1 \\ V_{BO} = ES_2 \\ V_{CO} = ES_3 \end{cases}$$

$$\begin{cases} S_1 = 1 & \text{si } k_1 \text{ fermé} & \text{si non} & S_1 = 0 \\ S_2 = 1 & \text{si } k_2 \text{ fermé} & \text{si non} & S_2 = 0 \\ S_3 = 1 & \text{si } k_3 \text{ fermé} & \text{si non} & S_3 = 0 \end{cases} \quad (34)$$

Finalement, we will have the following system:

$$\begin{bmatrix} V_{AN} \\ V_{BN} \\ V_{CN} \end{bmatrix} = \frac{E}{3} \begin{bmatrix} 2 & -1 & -1 \\ -1 & 2 & -1 \\ -1 & -1 & 2 \end{bmatrix} \begin{bmatrix} S_1 \\ S_2 \\ S_3 \end{bmatrix} \quad (35)$$

With:

$$E = U_{dc}$$

Using the functions of the connections on the inverter voltages are expressed as follows voltages

$$\begin{cases} V_{AB} = V_{AN} - V_{BN} = (S_1 - S_2)E \\ V_{BC} = V_{BN} - V_{CN} = (S_2 - S_3)E \\ V_{CA} = V_{CN} - V_{AN} = (S_3 - S_1)E \end{cases} \quad (36)$$

We can analyze all the possible states of the constituents of the inverter switches which eight (2^3) possible combinations six non-zero active states and two switching states equal zero.

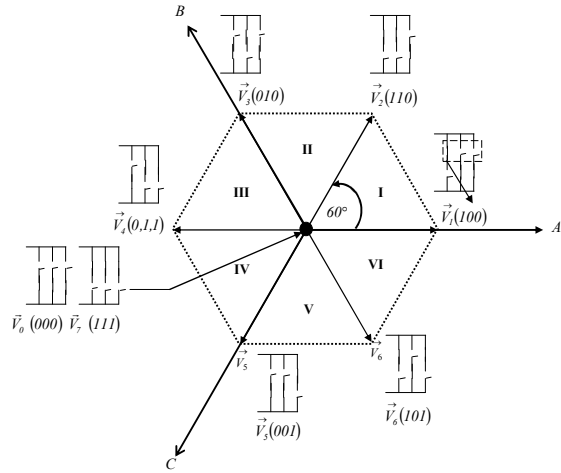


Fig. 5. Possible states of the constituents of the inverter switches

The table below shows the expressions that take the voltages and phase voltages, according to the open or closed state of the switches k1, k2, k3. (The states of k'1, k'2, k'3 are complementary to those of k1, k2, k3).

V_i	S_1	S_2	S_3	V_{AN}	V_{BN}	V_{CN}	V_{AB}	V_{BC}	V_{CA}
V_0	0	0	0	0	0	0	0	0	0
V_1	1	0	0	$2E/3$	$-E/3$	$-E/3$	E	0	$-E$
V_2	1	1	0	$E/3$	$-E/3$	$-2E/3$	0	E	$-E$
V_3	0	1	0	$-E/3$	$2E/3$	$-E/3$	$-E$	E	0
V_4	0	1	1	$-2E/3$	$E/3$	$E/3$	$-E$	0	E
V_5	0	0	1	$-E/3$	$-E/3$	$2E/3$	0	$-E$	E
V_6	1	0	1	$E/3$	$-2E/3$	$E/3$	E	$-E$	0
V_7	1	1	1	0	0	0	0	0	0

Table. 1 Voltages according to state of the switches k1, k2, k3

5. Prediction model

The numerical prediction model is mainly defined by input/output transfer function. The model is represented as CARIMA (Controlled Auto-Regressive Integrated Moving Average)

$$A(q^{-1})y(k) = B(q^{-1})u(k-d) + \frac{P(q^{-1})C(q^{-1})}{\Delta(q^{-1})} \quad (37)$$

We'll replace the output and the input of our machine with $C(q^{-1})=1$ and $P(q^{-1})=\xi(k)$

$$A(q^{-1})y(k) = B(q^{-1})\mathcal{V}(k-d) + \frac{\xi(k)}{\Delta(q^{-1})} \quad (38)$$

We conclude that for both active and reactive power

$$A(q^{-1})P_s(k) = B(q^{-1})\mathcal{V}_{qr}(k-d) + \frac{\xi(k)}{\Delta(q^{-1})} \quad (39)$$

$$A(q^{-1})Q_s(k) = B(q^{-1})\mathcal{V}_{dr}(k-d) + \frac{\xi(k)}{\Delta(q^{-1})} \quad (40)$$

$\Delta(q^{-1})=1-q^{-1}$ Ensure an integral action so it allows us to cancel any static error or a perturbation step; using this perturbation model is actually a consequence of the presence of load disturbances in step in many industrial processes. So we have zero static error against disturbances.

5.1. Cost function

The general purpose is to turn the future output error to zero with a minimum control effort. For example, the control law GPC is obtained by minimizing a quadratic criterion on future errors with a term weighting on the control increments

$$J_{GPC} = \sum_{N_1}^{N_2} \left[\hat{y}(k+j+d) - \omega(k+j+d) \right]^2 + \lambda \sum_{j=1}^{N_u} \Delta u^2(k+j) \quad (41)$$

$$J_{GPC} = \sum_{N_1}^{N_2} \left[\hat{P}_s(k+j+d) - P_{consigne}(k+j+d) \right]^2 + \lambda \sum_{j=1}^{N_u} \Delta V_{dr}^2(k+j) \quad (42)$$

$$J_{GPC} = \sum_{N_1}^{N_2} \left[\hat{Q}_s(k+j+d) - Q_{consigne}(k+j+d) \right]^2 + \lambda \sum_{j=1}^{N_u} \Delta V_{qr}^2(k+j) \quad (43)$$

5.2. Structure of the optimal predictor matrix

In this part of this paper we develop the calculation of the prediction of both active and reactive power $\hat{P}_s(k+j+d)$, $\hat{Q}_s(k+j+d)$ at time k to j ; to do that we must solve two Diophantine equations:

$$\Delta(q^{-1})A(q^{-1})J_j(q^{-1}) + q^{-d-j}F_j(q^{-1}) = 1 \quad (44)$$

5.2.1. Prediction of active power

We will use CARIMA model Eq.14 and the two Diophantine equations Eq.20 Eq.21 to define the prediction active power in terms of prediction control V_{dr} and polynomials single solutions $F_j(q^{-1}), H_j(q^{-1}), G_j(q^{-1}), J_j(q^{-1})$

$$P_s(k+d+j) = F_j(q^{-1})P_s(k) + H_j(q^{-1})\Delta V_{qr}(k-1) + G_j(q^{-1})\Delta V_{qr}(k+j-1) + J_j(q^{-1})\xi(k+d+j) \quad (45)$$

The noise will be supposed equal to zero

$$P_s(k+d+j) = F_j(q^{-1})P_s(k) + H_j(q^{-1})\Delta V_{qr}(k-1) + G_j(q^{-1})\Delta V_{qr}(k+j-1) \quad (46)$$

5.2.2. Prediction of reactive power

As we have done for active power we will define reactive power except for prediction control we use V_{qr} instead of V_{dr}

$$Q_s(k+d+j) = F_j(q^{-1})Q_s(k) + H_j(q^{-1})\Delta V_{dr}(k-1) + G_j(q^{-1})\Delta V_{dr}(k+j-1) \quad (47)$$

5.3. Predictive matrix representation

To represent the matrix active and reactive power prediction we must use some criterion as matrix like active power reference P_{sref} reactive power reference Q_{sref} the polynomials single solutions and of course both rotor voltages V_{qr} et V_{dr} .

$$P_{sref} = [P_{sref}(k+d+N_1), \dots, P_{sref}(k+d+N_2)]^T \quad (48)$$

$$Q_{sref} = [Q_{sref}(k+d+N_1), \dots, Q_{sref}(k+d+N_2)]^T \quad (49)$$

$$f(q^{-1}) = [F_{N_1}(q^{-1}), \dots, F_{N_2}(q^{-1})]^T \quad (50)$$

$$h(q^{-1}) = [H_{N_1}(q^{-1}), \dots, H_{N_2}(q^{-1})]^T \quad (51)$$

$$\tilde{V}_{qr} = [\Delta V_{qr}(k), \dots, \Delta V_{qr}(k+N_u-1)]^T \quad (52)$$

$$\tilde{V}_{dr} = [\Delta V_{dr}(k), \dots, \Delta V_{dr}(k+N_u-1)]^T \quad (53)$$

We conclude with the matrix optimal predictor for both powers:

$$\tilde{P}_s = G\tilde{V}_{qr} + f(q^{-1})P(k) + h(q^{-1})\Delta V_{qr}(k-1) \quad (54)$$

$$\tilde{Q}_s = G\tilde{V}_{dr} + f(q^{-1})P(k) + h(q^{-1})\Delta V_{dr}(k-1) \quad (55)$$

5.4. Future signal control expression

We can finally find the matrix expression of the two signals of command V_{qr} and V_{dr} by minimizing of

$$\text{cost function matrix } \frac{\partial J_P}{\partial \tilde{V}_{qr}} = 0 \quad \frac{\partial J_Q}{\partial \tilde{V}_{dr}} = 0$$

$$J_P = \left[G\tilde{V}_{qr} + fP_s(k) + h\Delta V_{qr}(k-1) - P_{sref} \right]^T \quad (56)$$

$$\left[G\tilde{V}_{qr} + fP_s(k) + h\Delta V_{qr}(k-1) - P_{sref} \right] + \lambda \tilde{V}_{qr}^T \tilde{V}_{qr}$$

$$J_Q = \left[G\tilde{V}_{dr} + fQ(k) + h\Delta V_{dr}(k-1) - Q_{sref} \right]^T \quad (57)$$

$$\left[G\tilde{V}_{dr} + fQ(k) + h\Delta V_{dr}(k-1) - Q_{sref} \right] + \lambda \tilde{V}_{dr}^T \tilde{V}_{dr}$$

That leads us to the optimal sequence of future control:

$$\tilde{V}_{qr} = [G^T G + \lambda I_{N_u}]^{-1} G^T [P_{sref} - f(q^{-1})P_s(k) - h(q^{-1})\Delta V_{qr}(k-1)] \quad (58)$$

$$\tilde{V}_{dr} = [G^T G + \lambda I_{N_u}]^{-1} G^T [Q_{sref} - f(q^{-1})Q_s(k) - h(q^{-1})\Delta V_{dr}(k-1)] \quad (59)$$

6. Simulation results

Modeling the turbine, machine and GPC controller has been implemented in the MATLAB environment Simulink to conduct tests of our control, so we submitted this system on echelons of active and reactive power to observe the behavior of the predictive control.

Parameters for our DFIG are:
 $p=2$ pair of pole, $R_s=5\Omega$, $R_r=0.5\Omega$, $M=0.034H$,
 $L_m=0.08H$, $L_r=0.4H$, $L_s=0.07H$, $\omega_s=314$, $g=0.03$,
 $J=1000 \text{ kg.m}^2$, $f=0.0024\text{kg/s}$

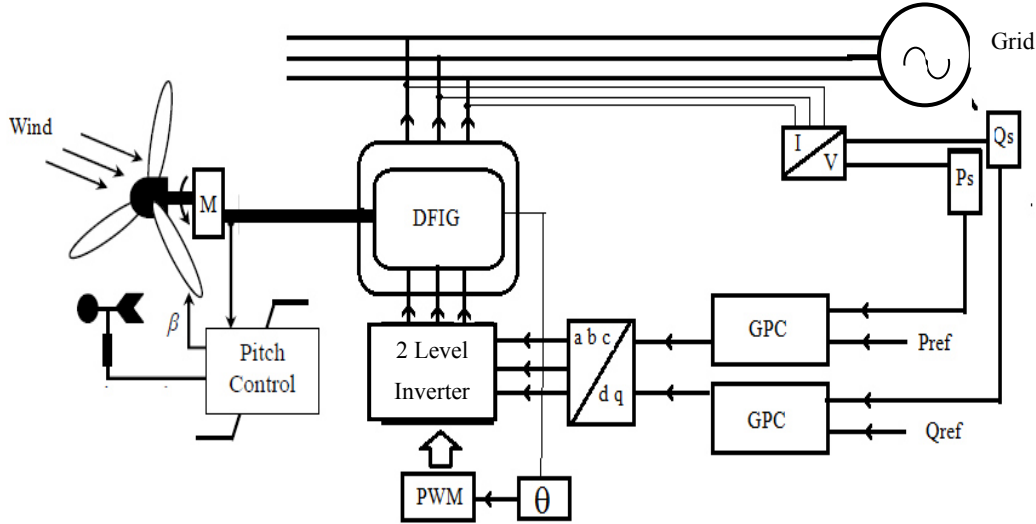


Fig. 6. Block diagram of the whole system

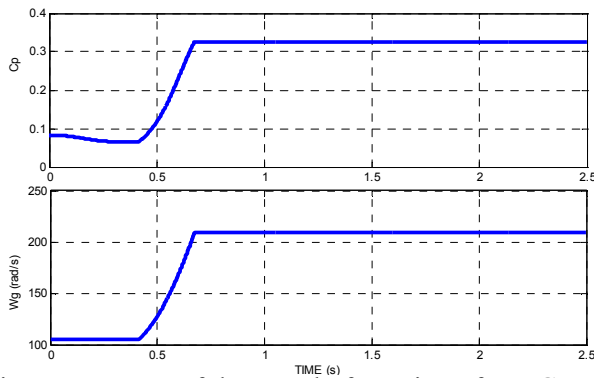


Fig. 7. Response of the speed of rotation of DFIG and power coefficient C_p

Figure (7) shows us that batch control maximizes the response of C_p that implies of Ω_g

The corrector GPC for active power can be

synthesized with the set of parameters:

$$N_1 = 1; N_2 = 31, N_u = 2, \lambda = 44$$

And for reactive power

$$N_1 = 1; N_2 = 30, N_u = 2, \lambda = 53$$

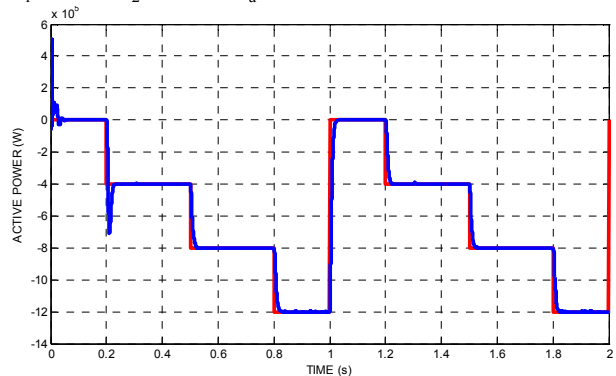


Fig. 8. Response of the active power by GPC control

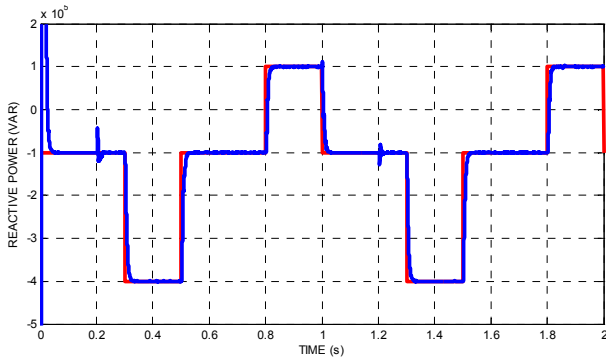


Fig. 9. Response of the reactive power by GPC control

We can see from the two responses of active and reactive power represented in the two figures (8) and (9) that the echelons of power are followed by the generator for both the active and reactive power and a dynamic that reacts quickly and without overshoot; the function of reactive power control allows us to have a negative reactive power capacitive or positive inductive behavior and we observe that there is no coupling effect between the two control axes d and q for the two powers.

We observe the effect of coupling between the two control axes d and q as the echelon of active power has changed induced low overshoot on reactive power in $t=0.2s$, $t=1s$ and $t=1.2$ also when reactive.

We note an overshoot because startup in response of reactive power we can eliminate this overshoot by using power limiter to the input of our system for example a rheostat

We also notice small oscillation in response of active power in the intervals $[0.2; 0.4]$ and $[0.8; 1]$ and $[1.8; 2]$ and even reactive power in the interval $[0.3; 0.5]$ $[1.3; 0.4]$ $[1.8; 2]$ because of the PWM control of the inverter.

6. Robustness test

We will try to see the response of active and reactive power even after changing parameter of DFIG, so we will change resistance and inductance of 20% of its nominal values.

The results, represented in figures 10 and 11, show that generalized predictive control is robust against parameter changes because, even changing resistance and inductance, the response is the same as the first response in figures 8 and 9.

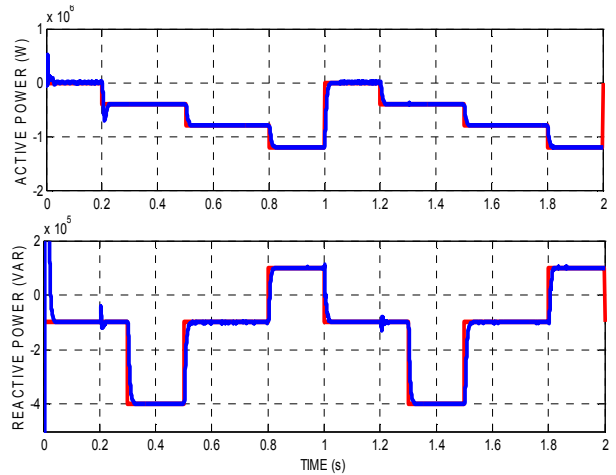


Fig. 10. Response of the active and reactive power by GPC control with changing of resistance 50%

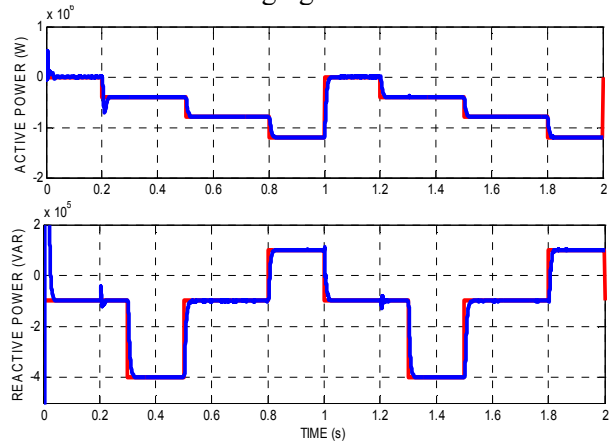


Fig. 11. Response of the active and reactive power by GPC control with changing of inductance 50%

7. Conclusion

In this paper we studied predictive control for induction machine dedicated for a wind turbine which is robust even after the internal parameters changes as resistance and inductance of the DFIG because our regulator changes alternately rotoric voltages in real time after the prediction of the active and reactive power that should be.

Nomenclature

$V_{ds}, V_{qs}, V_{dr}, V_{qr}$: Two-phase statoric and rotoric voltages; $\phi_{qs}, \phi_{ds}, \phi_{qr}, \phi_{dr}$: Statoric and rotoric flux ; θ_s : the electrical angle of the rotating field stator; θ_r : the electrical angle of the rotating field rotor; R_s, R_r : phase statoric and rotoric resistances; M : Magnetizing inductance; L_s, L_r : Total cyclic statoric and rotoric inductances; g : generator slip; J : Inertia J_t : Inertia of turbine J_g : Inertia of generator f : viscous friction; f_t : viscous friction of turbine, f_g : viscous friction of generator ; C_t : The torque of the turbine; C_g : The torque of the generator; G : gain of the speed

multiplier. C_f : viscous friction torque ω_s : The angular speed; C_{em} : The electromagnetic torque; C_r : The resistant torque; Ω : The speed of rotation of the axis of the DFIG; C_p : power coefficient; λ : relative speed; β : pitch angle; R : radius of turbine; V : wind speed; Ω_t : turbine speed; Ω_g : generator speed; ρ : air density β_{opt} optimum pitch angles α_{opt} : optimum angle of incidence

References

1. Boyette, *Contrôle-commande d'une GADA avec système de stockage pour la production éolienne*, Thèse de Doctorat, Université Henry Poincaré, Nancy I, (2006).
2. Y. Djeriri, A. Meroufel, A. Massoum, and Z. Boudjema; *A comparative study between field oriented control strategy and direct power control strategy for DFIG*, Journal of Electrical Engineering JEE.
3. Zongkai, Shao.; Yuedong, Zhan.; Youguang, Guo. *Fuzzy neural network-based model reference adaptive inverse control for induction machines Applied Superconductivity and Electromagnetic*. (ASEMD) International Conference (2009).
4. Xingjia, Yao.; Hongxia, Sui.; Zuoxia, Xing. *The Dynamic Model of Doubly-fed Induction Generator Based on Wind Turbine*. (IEEE) International Conference (2007).
5. Ronghui Zhou; Tong Zhao; Yong Li; Xiangming Shen, *A design scheme of model reference adaptive control system with using a smooth parameter projection adaptive law*; (2012).
6. Akkari, Nadia. *Commande Adaptative de la Machine Asynchrone a Double Alimentation par des sources de tension*. Mémoire de Magister en Electricité Industrielle, Université de Batna (2005).
7. Singh, G. K.; Nam, K. *A Simple Indirect Field-Oriented Control Scheme for Multiphase Induction Machine*, IEEE Trans. Ind Appl 52, pp. 1177–1184. (2005).
8. Clarke, D.W.; Mohtadi, C; Tuffs, P.S. *Generalized predictive control*, parts 1 and 2, Automatica 23, pp. 137–160 (1987).
9. Richalet, J.; Rault, A.; Testud J.L. *Model Predictive Heuristic Control: applications to industrial processes*, Automatica, 14, pp. 413–428 (1978).
10. Zare, M.; Niasar, A.H.; *A novel sensorless vector control of hysteresis motor drive*; IEEE Publication Year: (2013).
11. Gallah, T.; Khedher, A.; Mimouni, M. F.; M'sahli, F. *Theoretical comparison between Field Oriented and Generalized Predictive Control for an Induction Motor*, Int. Journal on Sciences and Techniques of Automatic control (2007).
12. Kwon, W.H.; Han, S. *Receding Horizon Control*, Springer Press, UK (2005).
13. Ramdane Amel, *Commande par EMCS d'une Machine à Induction Alimentée par un convertisseur de Fréquence*, Mémoire de Magister en Electrotechnique, Université de Batna (2004).
14. F. POITIERS, *Etude et commande de génératrices asynchrones pour l'utilisation de l'énergie éolienne*, Thèse de Doctorat de l'Université de Nantes, (2003)
15. Boucher, P.; Dumur, D. *La Commande Prédictive*, Edition Technip, Paris. (2000).
16. K. MOUILAH*, M. ABID, A.NACERI, M.ALLAM, *Fuzzy control of a doubly fed induction generator for Wind turbines*, Journal of Electrical Engineering JEE.
17. H. Abouobaida, M. Cherkaoui, *Wind energy conversion system, Modeling and Control of Doubly Fed Induction (DFIG)*, Journal of Electrical Engineering JEE.
18. I. Hamzaoui, F. Bouchafaa and A. Talha, *pitch angle control for variable speed wind turbines with doubly fed induction generators* Journal of Electrical Engineering JEE.
19. HOUARI. KHOUIDMI AHMED. MASSOUM, *generalized predictive speed controller of double stator induction motor*, Journal of Electrical Engineering JEE.
20. Springer book, *Advanced textbooks in control and signal processing, Model predictive control*, Octobre (2014)
21. Qiao Zhang, Member, IEEE, Run Min, Qiaoling Tong, Member, IEEE, Xuecheng Zou, Zhenglin Liu, and Anwen Shen, *Sensorless Predictive Current Controlled DC-DC Converter With a Self-Correction Differential Current Observer*, IEEE transactions on industrial electronics, vol. 61, no. 12, december (2014)
22. Mads r. Almassalkhi, member, IEEE, and ian a. Hiskens, fellow, ieee, *Model-predictive cascade mitigation in electric Power systems with storage and renewables—part 1: Theory and implementation*, IEEE transactions on power systems, vol. 30, no. 1, january (2015)
23. S. Heier, *Grid Integration of Wind Energy Conversion Systems*, John Wiley & Sons, 2006.
24. K. M. Moudgalya, *Generalized Predictive Control, CL 692 Digital Control*, IIT Bombay.2001.
25. K. M. Moudgalya, , *CL 692 Digital Control*, IIT Bombay.2001.
26. Mihai Draganescu, Shen Guo, Jacek Wojcik, *Generalized Predictive Control for Superheated Steam Temperature Regulation in a Supercritical Coal-fired Power Plant*, CSEE journal of power and energy systems, vol. 1, no. 1, march 2015.